Pure appl. geophys. 152 (1998) 781–809
0033–4553/98/040781–29 $ 1.50 + 0.20/0

Pure and Applied Geophysics

Numerical Simulation of the Sensitivity of Summer Monsoon Circulation and Rainfall over India to Land Surface Processes

S. RAMAN,[1] U. C. MOHANTY,[2] N. C. REDDY,[1] K. ALAPATY[1] and R. V. MADALA[3]

Abstract—The influence of soil moisture and vegetation variation on simulation of monsoon circulation and rainfall is investigated. For this purpose a simple land surface parameterization scheme is incorporated in a three-dimensional regional high resolution nested grid atmospheric model. Based on the land surface parameterization scheme, latent heat and sensible heat fluxes are explicitly estimated over the entire domain of the model. Two sensitivity studies are conducted; one with bare dry soil conditions (no latent heat flux from land surface) and the other with realistic representation of the land surface parameters such as soil moisture, vegetation cover and landuse patterns in the numerical simulation. The sensitivity of main monsoon features such as Somali jet, monsoon trough and tropical easterly jet to land surface processes are discussed.

Results suggest the necessity of including a detailed land surface parameterization in the realistic short-range weather numerical predictions. An enhanced short-range prediction of hydrological cycle including precipitation was produced by the model, with land surface processes parameterized. This parameterization appears to simulate all the main circulation features associated with the summer monsoon in a realistic manner.

Key words: Numerical simulation, summer monsoon, circulation, land surface, parameterization.

1. Introduction

The summer monsoon is an important circulation over south Asia for three to four months from June to September every year. This monsoon is accompanied with heavy precipitation over the Indian subcontinent. The onset of the monsoon as well as space time variations in the monsoon activity and rainfall, fluctuate from year to year. Surface-temperature differences between land and sea produce circulations which trigger the onset of convection and monsoon activity over the region. The monsoon varies widely in space and time which makes it difficult to

[1] Department of Marine, Earth and Atmospheric Sciences, North Carolina State University, Raleigh, NC 27695-8208, U.S.A.

[2] Centre for Atmospheric Sciences, Indian Institute of Technology, New Delhi, India.

[3] Naval Research Laboratory, Washington, D.C., U.S.A.

predict its activity on a day-to-day basis. Another factor that causes heavy rainfall along the west coast and northeast India is orographic lifting which triggers deep convection in these regions. Consequently, the establishment and maintenance of the summer monsoon is considered to be the result of complex land-air-ocean interaction processes over the region. Though several studies have been conducted on the numerical simulation of the southwest monsoon, only a limited number of them have considered the role of land-surface processes such as vegetation cover and soil moisture on mesoscale distribution of monsoon rainfall over India.

The role of land-surface processes in simulation of atmospheric circulation is examined by various land-surface parameterization schemes (SELLERS *et al.*, 1986; DICKENSON *et al.*, 1986; HENDERSON-SELLERS, 1993; NOILHAN and PLANTON, 1989). The importance of land-surface characteristics in generating mesoscale circulations has been recognized in recent years. The most widely studied phenomenon is the atmospheric response associated with differences in soil moisture availability with no vegetation cover. ZHANG and ANTHES (1982) demonstrated that variations in soil moisture can cause significant effects on the boundary layer characteristics. OOKOUCHI *et al.* (1984) showed that differential heating associated with variations in soil moisture can produce circulations similar to a sea breeze type of circulation. MAHFOUF *et al.* (1987) also obtained similar results considering two soils of different textures, although with the same relative moisture content. They concluded that soil texture substantially influences surface moisture availability. Further, they found that inhomogeneities in soil moisture on a horizontal scale of 100–200 km can initiate rainfall in a convectively unstable environment with sufficient moisture, in the absence of any significant synoptic flow.

The mesoscale response to variations in vegetation characteristics has been given only modest attention. The presence of vegetation tends to modify the surface thermal fluxes as compared to those of an equivalent bare soil surface under the same environmental conditions. Thus, the partitioning of thermal energy between the sensible and latent heat fluxes is likely to be different for the two surfaces. Mesoscale circulations such as sea breezes or thermally induced upslope flows are directly related to the magnitude and the horizontal distribution of the surface sensible heat fluxes. The characteristics of these circulations are likely to be modified in the presence of vegetation as compared to bare soil conditions.

Previous observational studies (BURMAN *et al.*, 1977; BARNSTON and SCHICKEDANZ, 1984) documented the development of convective clouds and subsequent precipitation near the transition zone between the vegetated area and the bare soil. Numerical modeling studies (MCCUMBER, 1980; ANTHES, 1984; HONG *et al.*, 1995; XU *et al.*, 1996) also indicated a significant increase in convective rainfall in the vegetated area. GARRETT (1982) concluded that the transpiration from the vegetated area may affect the formation of convective clouds and rainfall through their effect on the boundary layer growth. MAHFOUF *et al.* (1987) indicated significant low-level convergence and convection in the transition zone between

bare soil and vegetation covered soil. OTTERMAN (1974) concluded that vegetated surfaces in regions of marginal rainfall would be more conducive to convective precipitation than a bare soil surface. The increase in convective rainfall would occur through increased low-level moisture from evapo-transpiration, decreased wind speed, and increased turbulent mixing. Therefore, the role of land-surface processes (LSP) on the production of mesoscale circulation and convection is well recognized.

This paper is an attempt to examine the influence of soil moisture and vegetation variations on the simulation of summer monsoon circulation and associated rainfall over India. For this purpose, a simple soil moisture and vegetation parameterization scheme proposed by NOILHAN and PLANTON (1989) has been incorporated in a high-resolution three-dimensional regional model.

2. The Mesoscale Model

The details of Naval Research Laboratory/North Carolina State University (NRL/NCSU) model used in the present study are provided in a NRL memorandum report by MADALA *et al.* (1987). This is a primitive equation model in terrain following coordinate ($\sigma = p/p_s$) with a staggered horizontal grid network (known as Arakawa C-grid) in a general curvilinear coordinate system. The continuous governing equations are written in flux form. Physics included in the model are convective and nonconvective precipitation, and atmospheric boundary layer processes. Atmospheric radiation is not considered in this experiment because of the relatively short period of the model integration time, extending to 48 hours. Convective precipitation is parameterized using a modified Kuo scheme (KUO, 1974; ANTHES, 1977). Nonconvective precipitation occurs in the model when super saturation is reached on the resolvable scale. Excess moisture precipitates into lower model layers and evaporates or falls to the surface. A dry convective adjustment scheme which conserves total static energy is included in the model above the atmospheric boundary layer to remove superadiabatic lapse rates.

The time integration in this model involves a split-explicit method which allows a larger time step by effectively separating various terms in the prognostic equations into parts governing slow-moving Rossby modes and fast-moving gravity modes. For the first and second fast-moving gravity modes smaller time step is used, and for all other modes a larger time step is applied. The implementation of these varying time steps is the basis for the split-explicit method. The time steps for the slow moving modes in the coarse grid model and the fine grid model are 300 s and 100 s, respectively, and appropriate smaller time steps which satisy CFL (Courant, Frederick and Louis) criterion are used for the fast-moving modes. For further details the reader is referred to MADALA *et al.* (1987). For the horizontal differencing, a staggered grid (Arakawa C-grid) is used with p_s, q, T, ϕ, and $\dot{\sigma}$, specified at

the same horizontal points, and u and v interlaced between them where p_s is the surface pressure, q the specific humidity, T the temperature, ϕ the geopotential, $\dot{\sigma}$ the vertical velocity, u the zonal wind velocity, and v the meridional wind velocity, respectively. The finite-difference technique used in the model is second-order accurate. It conserves total energy, mass and momentum in the absence of the heat and momentum sources.

In the present study a one-way interactive nested grid (double nest) version of the model is used (ALAPATY *et al.*, 1995). The fine grid model is nested into the coarse grid model such that every third grid in the fine grid is collated with that in the coarse grid. The domains of simulation in the Coarse-Grid Mesh (CGM) and the Fine-Grid Mesh (FGM) are shown in Figure 1a. The CGM covers most of monsoon region from 37.5°E to 112.5°E in the east-west direction and 42.5°N to 20.5°S in the north-south direction with a horizontal resolution of 1.5 degree latitude/longitude. The FGM is located over India and the surrounding seas from 54°E to 102°E in east-west direction and 30.5°N to 5.5°S in north-south direction, with a horizontal resolution of 0.5 degree latitude/longitude. The nested grid is positioned so that its boundary rows and columns overlap the coarse grid model interior rows and columns. This nesting configuration enables the fine grid mesh domain boundary values to be specified by the coarse grid mesh interior grid points.

The model surface topography was derived from the U.S. Navys' 10′ global topography data. Figure 1b delineates the fine grid model topograpy. Large surface elevation over the northern region are the Himalayan mountains with a maximum height of 6.8 km. Western Ghats are located along the west coast of India. The Western Ghat mountains extend about 1600 km in north-south direction with average heights of 800 m and individual peaks slightly higher (reaching 1100 m). The Western Ghat mountains are about 100 km inland in the fine grid domain (two grid points) and 150 km inland in the coarse grid domain (one grid point). In the fine domain mountain heights are higher and steeper as compared to the coarse domain, due to the fine resolution of the domain. In the vertical the model has finer resolution within the boundary layer (8 layers in the lowest 2000 m) and the next 8 layers are above the boundary layer with a total of 16 layers. The model σ levels and corresponding pressures are given in Table 1. The model top is at about 100 hPa ($\sigma = 0.1$). The sea-surface temperatures (SST) were obtained from the operational analysis of the National Center for Environmental Prediction (NCEP) and used as surface condition over water bodies. The SST was kept constant during the model integration.

3. Experimental Design

The main objective of this study is to investigate the effects of the land-surface processes such as soil moisture and vegetation cover on the simulation of monsoon

circulation and associated rainfall. For this purpose, two experiments are designed. In the first experiment, bare and dry soil conditions are used in the atmospheric model, henceforth referred to as DRY case. In the second experiment, a simplified land-surface process parameterization (NOILHAN and PLANTON, 1989) is coupled to the atmospheric model, hereafter referred to as MOIST case. The three-dimensional NRL/NCSU mesoscale model is used for both simulations. All the simulation integrations are carried out up to 48 hrs, starting from the initial condition of 12 UTC on 12 July, 1988.

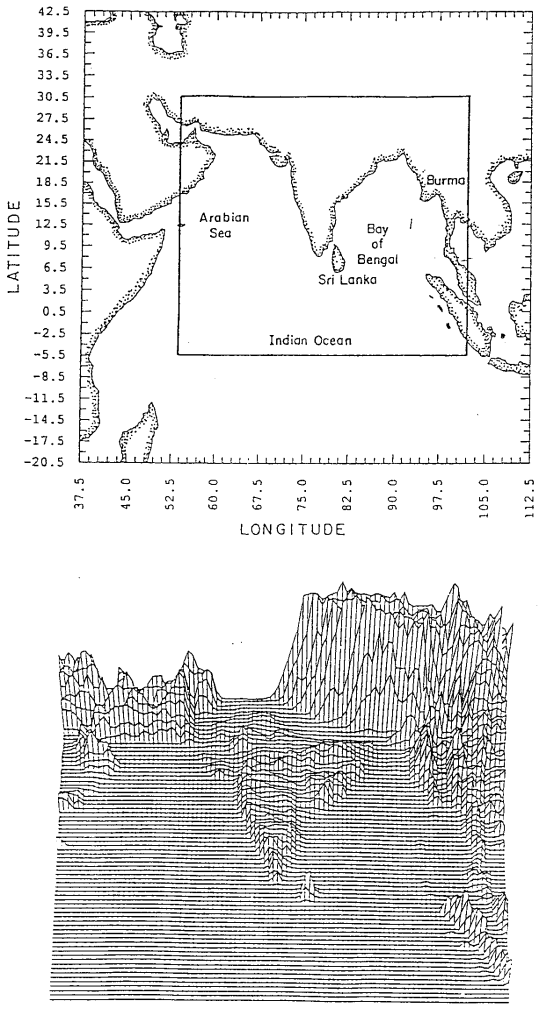

Figure 1
(a) Simulation domain, the inner box is the fine mesh domain (FGM) and the outer box is the coarse domain (CGM) and (b) topography in fine grid mesh domain.

Table 1

Model σ levels and corresponding pressures for a surface at 1000 hPa

Model layer k	Sigma level σ	Pressure level p (hPa)
1	0.05	50
2	0.15	150
3	0.25	250
4	0.35	350
5	0.45	450
6	0.55	550
7	0.65	650
8	0.75	750
9	0.82	820
10	0.86	860
11	0.90	900
12	0.935	935
13	0.96	960
14	0.9775	977
15	0.99	990
16	0.9975	997

The simulation with the DRY experiment, which considers dry bare soil conditions, has zero latent heat flux over land surface. The MOIST case explicitly estimates the latent heat flux over land. Several surface parameters are required for the MOIST case simulation. The surface parameters such as surface roughness (z^0), vegetation cover (Fig. 2a), leaf area index (LAI, Fig. 2b), soil types (11 types, Table 2) with critical moisture content parmeters as obtained by CLAPP and HORNBERGER (1978). Albedo, stomatal resistance, percentage of radiation intercepted by foliage, and the landuse categories were obtained from various global $1° \times 1°$ latitude/longitude data archives at the National Center for Atmospheric Research (MATTHEWS, 1984). The initial soil moisture (Fig. 2c) was obtained from available climatological soil moisture data which is dependent on landuse patterns (Table 3). Soil types were also obtained from the National Center for Atmospheric Research (NCAR) data sets and are shown in Figure 2d.

Initial conditions used in this study are interpolated from the European Center for Medium Range Weather Forecasting (ECMWF) operational analyses available at 14 mandatory vertical pressure levels with 1.875° Longitude/Latitude horizontal resolution. These data are interpolated to model grid points in the coarse and fine grid domains.

Monsoon activity was moderately active over the Indian subcontinent during the simulation period, from 12 UTC 12 July to 12 UTC 14 July, 1988. During this period wide-spread rainfall occurred over central India. On 14 July, 1988, rainfall occurred over most of India. This case was considered to be a suitable one to study

the role of land surface parameterization on monsoon simulation, employing a mesoscale model because of the widespread occurrence of rainfall.

4. Results and Discussion

In this section, results from the numerical simulations using dry soil conditions (DRY) and interactive soil moisture scheme (MOIST) are presented and compared

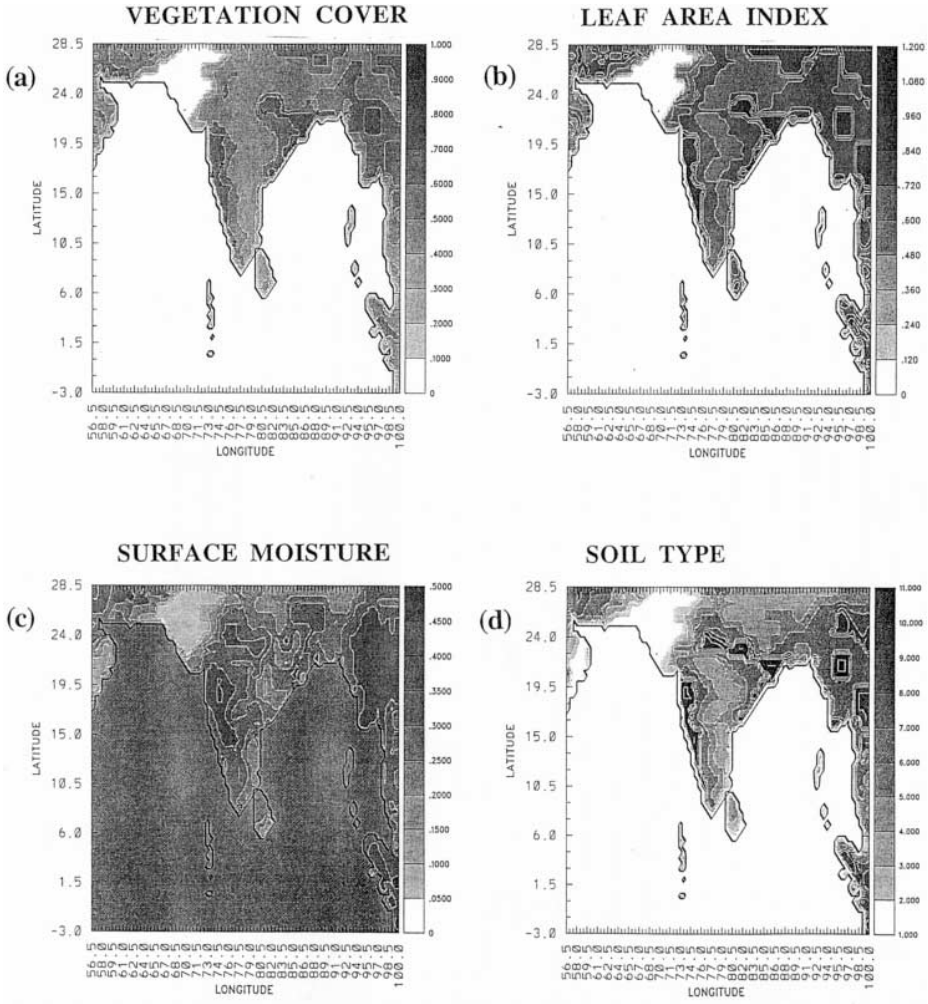

Figure 2
Initial input used in the fine grid model (a) vegetation cover, (b) leaf area index, (c) soil moisture and (d) soil types (Source NCAR data archives).

Table 2

Critical water contents of soils derived from the classification of CLAPP *and* HORNBERGER *(1978): Saturated moisture w_{sat}, field capacity w_{fc}, wilting point w_{wilt} are given in volumetric percentage*

Soil type	w_{sat}	w_{fc}	w_{wilt}
Sand	0.395	0.135	0.068
Loamy sand	0.410	0.150	0.075
Sandy loam	0.435	0.195	0.114
Silt loam	0.485	0.255	0.179
Loam	0.451	0.240	0.155
Sandy clay loam	0.420	0.255	0.175
Silty clay loam	0.477	0.322	0.218
Clay loam	0.476	0.325	0.250
Sandy clay	0.426	0.310	0.219
Silty clay	0.482	0.370	0.283
Clay	0.482	0.367	0.286

with the observations when possible. The primary difference in these two simulations is the way in which evaporation flux (latent heat flux) is estimated over land.

Both the experiments (DRY and MOIST) were preformed for 48 h period starting from the initial condition of 12 UTC 12 July, 1988. Results of Day-1 and Day-2 were examined in detail and compared with the available observations/analysis. However, for brevity, only the model results at 48 hrs integration are presented here. The coarse grid model was used primarily to capture the large-scale circulations associated with the monsoon flow and also to provide the boundary conditions for the fine grid model. Since the available ECMWF analysis is of coarse resolution (1.875° latitude/longitude), the monsoon circulation and associated features (monsoon trough, Somali jet, upper level easterly jet, etc.) are to some

Table 3

Land use categories and their corresponding soil moisture used in the model

	Land use category	Soil moisture
0	Water	1.0
1	Mixed farming/cultivated land	0.3
2	Grassland/evergreen shrub land	0.4
3	Meadow and shrub land	0.35
4	Evergreen forest	0.5
5	Mixed deciduous forest	0.3
6	Deciduous forest	0.3
7	Tropical evergreen forest	0.5
8	Woodlands tall grass	0.15
9	Desert	0.01
10	Tundra	0.5
11	Permanent ice	0.95

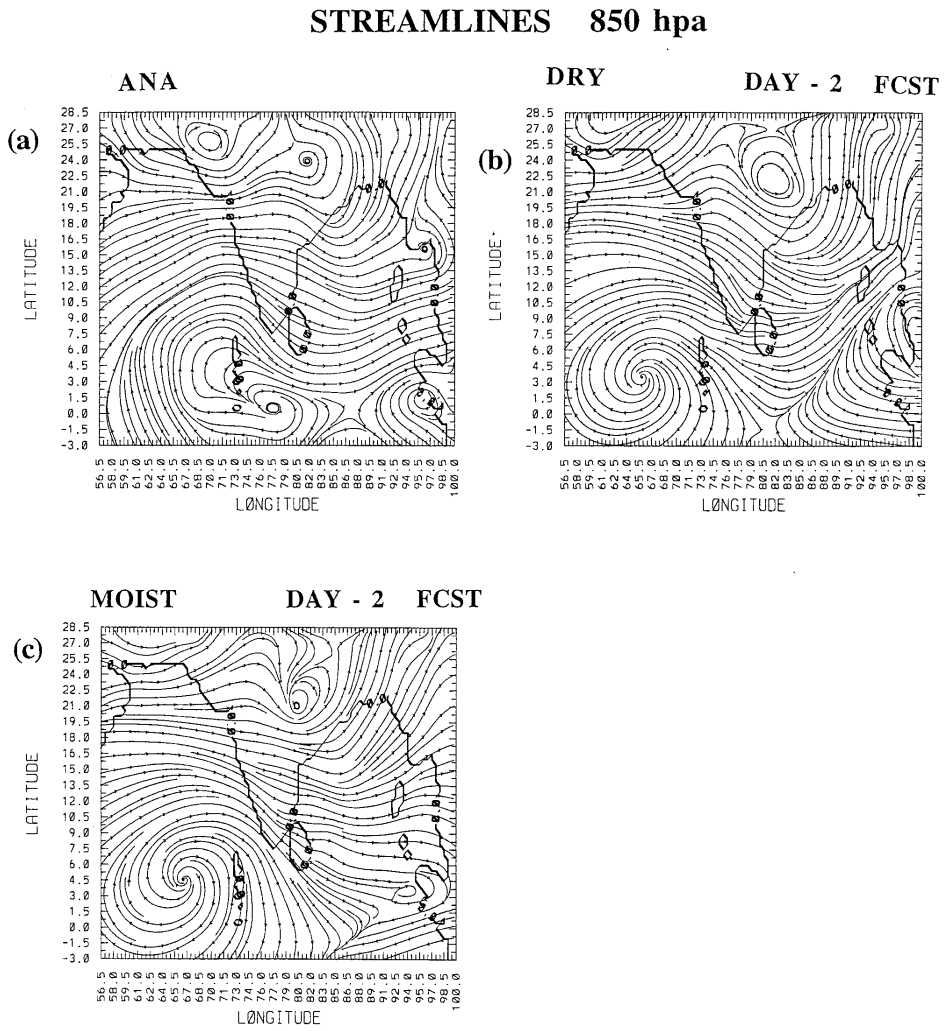

Figure 3
Horizontal streamline distribution for fine mesh domain at 850 hPa at 12 UTC on 14 July, 1988 for (a) ECMWF analysis, (b) Day-2 simulation DRY case and (c) Day-2 simulation MOIST case.

extent weaker in the initial conditions. Further, though the results from both the CGM and the FGM were examined in detail, most of the discussions presented here pertain to FGM results.

4.1 Monsoon Circulation Features

Analyzed ECMWF horizontal streamline distribution at 850 hPa for the fine grid model at 12 UTC on 14 July is shown in Figure 3a. It serves as a verifying

analysis for two days of model simulation beginning from 12 UTC of 12 July, 1988. The cyclonic circulations over eastern India are due to the presence of a low-pressure system in that region. Strong heating in the desert regions leads to the formation of a heat low in northwest India. Simulated horizontal streamline patterns for the DRY and MOIST cases are presented in Figures 3b and 3c, respectively. Streamline patterns are well simulated in the model and are consistent with the respective ECMWF analysis of wind as well as geopotential distributions over the regions of low pressure and the heat low (not shown). Streamline simulation shown for the MOIST case in Figure 3c clearly indicates a closed circulation over the eastern sector of the monsoon trough, consistent with the verifying analysis, while the simulation in the DRY case indicates more intense circulation over the eastern sector of the monsoon trough. Both simulations tend to weaken the heat low over the western sector of the monsoon trough.

An important low-level feature usually observed during the south-west monsoon is the Somali jet over the Arabian Sea at about 850 hPa. The wind speed distribution at 850 hPa of the verifying analyses and the fine grid DRY and MOIST model Day 2 simulations at 12 UTC on 14 July are illustrated in Figures 4a, 4b and 4c, respectively. The presence of Somali jet, indicated by strong winds off the east coast of Africa, can be clearly seen from Figures 4a, 4b and 4c. However, the Somali jet is decidedly stronger in model predictions (Figs. 4b and 4c) as compared to the ECMWF operational analysis (Fig. 4a). Increased convection over land for the MOIST simulations causes release of latent heat in mid-troposphere which in turn intensifies the horizontal temperature gradients, resulting in an increase in the low-level circulation and the intensity of the Somali jet. The maximum wind speeds along the Somali jet are 25.7 m s^{-1}, 31.6 m s^{-1} and 34.8 m s^{-1} for the ECMWF analyses, DRY and MOIST simulations, respectively. Lower values of the ECMWF analysis could be due to its coarser resolution. Results for the coarse grid model (not shown) also indicate the Somali jet in the same location as the fine grid model, however the winds are relatively weaker (DRY = 15.8 m s^{-1} and MOIST = 16.9 m s^{-1}). This is obviously due to the coarser horizontal resolution.

The verifying analysis and the predicted fields indicate intensification of the winds along the Somali jet on the second day, as compared to the first day (not shown). An overall increase of about 3–5 m s^{-1} in both the analysis and the predicted wind fields on the second day of simulation (Fig. 4, on 14 July) are apparent. This increase in wind speed leads to an enhancement of surface latent and sensible heat fluxes along the jet on the second day (discussed later). Winds intensified due to the occurrence of an active monsoon condition over India during this period (12–18 July, 1988).

Another prominent feature during the southwest monsoon is the Tropical Easterly Jet (TEJ) which forms as part of the return flow at about 150 hPa. It is a semi-permanent circulation feature associated with the Asian summer monsoon. The spatial distribution of wind speed at 150 hPa for the ECMWF analysis and the fine grid model simulation with DRY and MOIST cases at 12 UTC on 14 July are

presented in Figures 5a, 5b and 5c, respectively. The ECMWF analysis (Fig. 5a) shows a wind maximum of about 44 m s^{-1}. This wind maximum at 150 hPa is associated with the TEJ. Both the model runs (DRY and MOIST) could simulate this tropical easterly jet; however, the wind speed distribution in the MOIST case is closer to the verifying analysis. The maximum wind speed along the TEJ with DRY (Fig. 5b) and MOIST (Fig. 5c) model run are 37.8 m s^{-1} and 45.8 m s^{-1},

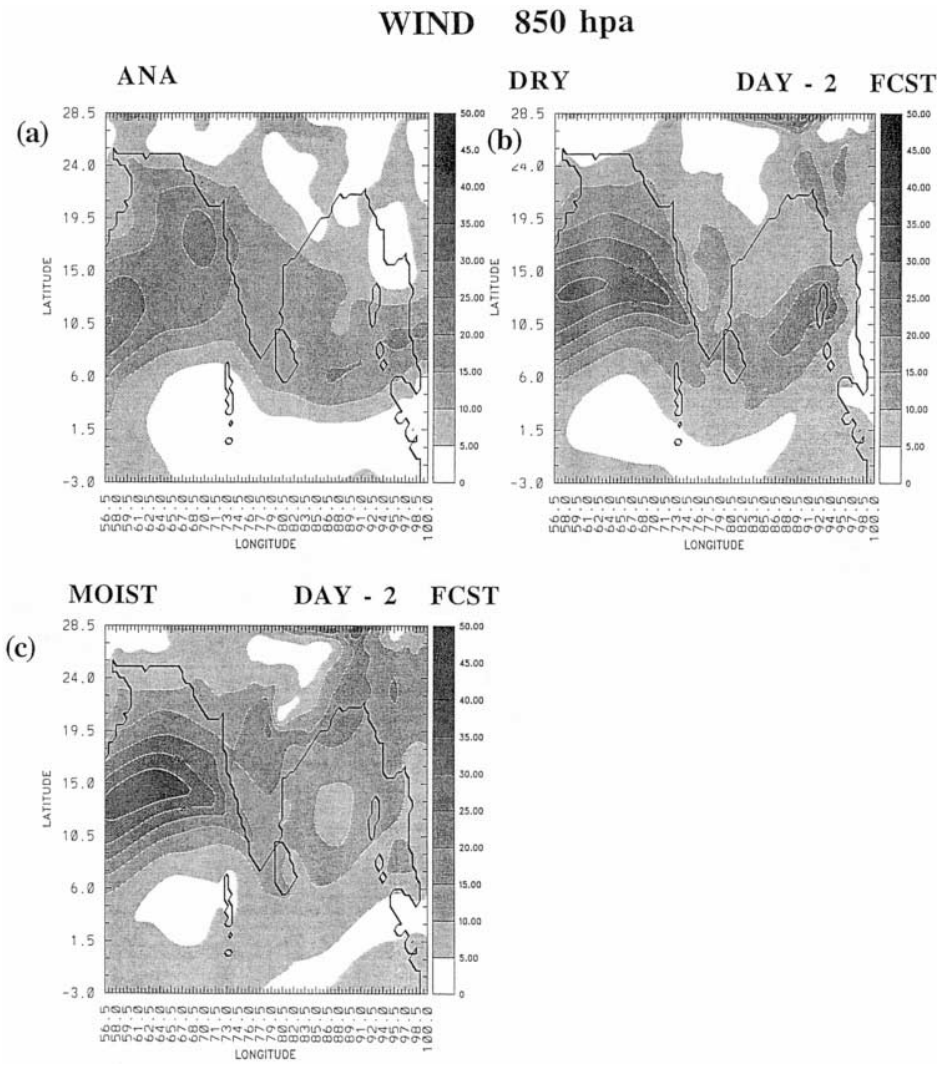

Figure 4
Horizontal wind speed (ms^{-1}) for fine mesh domain at 850 hPa at 12 UTC on 14 July 1988 for (a) ECMWF analysis, (b) Day-2 simulation DRY case and (c) Day-2 simulation MOIST case.

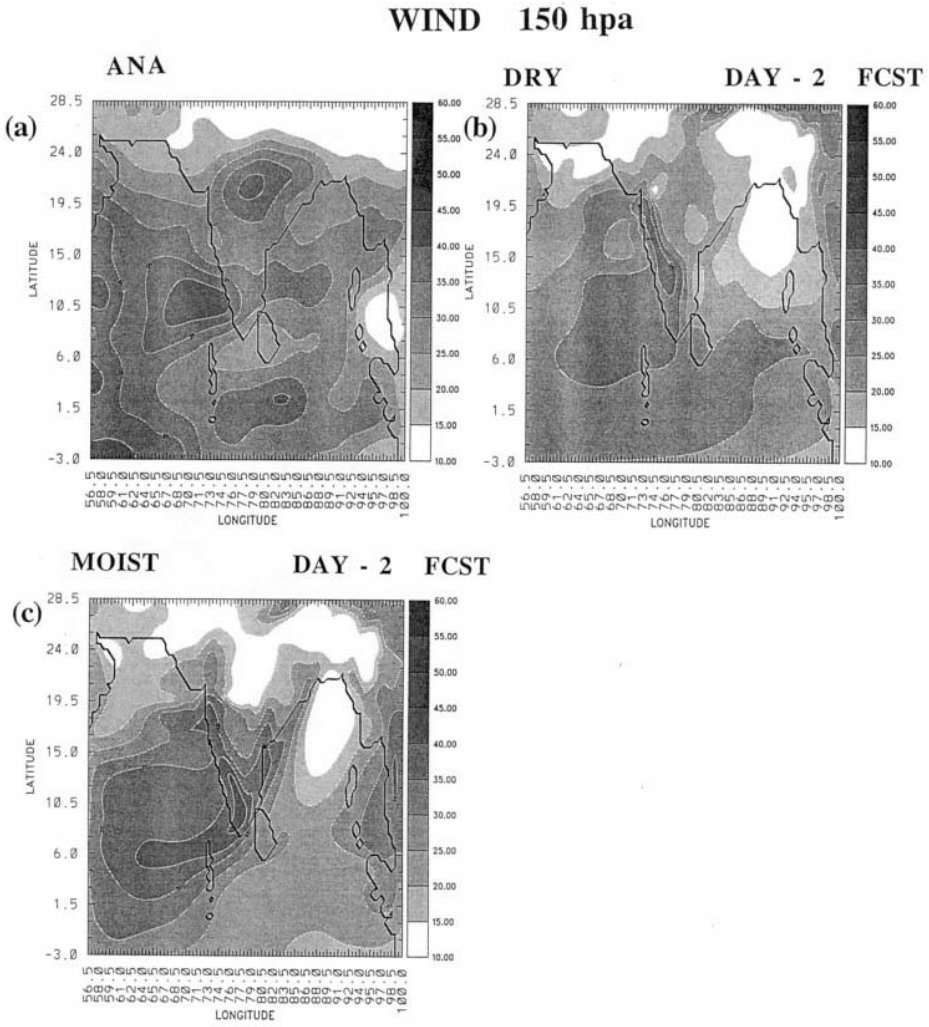

Figure 5
Horizontal wind speed (ms^{-1}) for fine mesh domain at 150 hPa at 12 UTC on 14 July, 1988 for (a) ECMWF analysis, (b) DRY case and (c) MOIST case.

respectively. Thus the results with the MOIST case appear to be more realistic and close to the ECMWF analysis in simulating the observed strength of the jet. An increase in the strength of the tropical easterly jet is again associated with an increase in the convection over land for the MOIST case and an increase in low-level circulation as discussed before. This is consistent with larger vertical motions over land for the MOIST case as will be shown later.

It would be of interest to examine the vertical structure of both these jets. For this purpose, latitude-height cross section of the sectorial mean (56.5°E–100°E) zonal winds on 14 July are shown in Figures 6a, 6b and 6c for the ECMWF

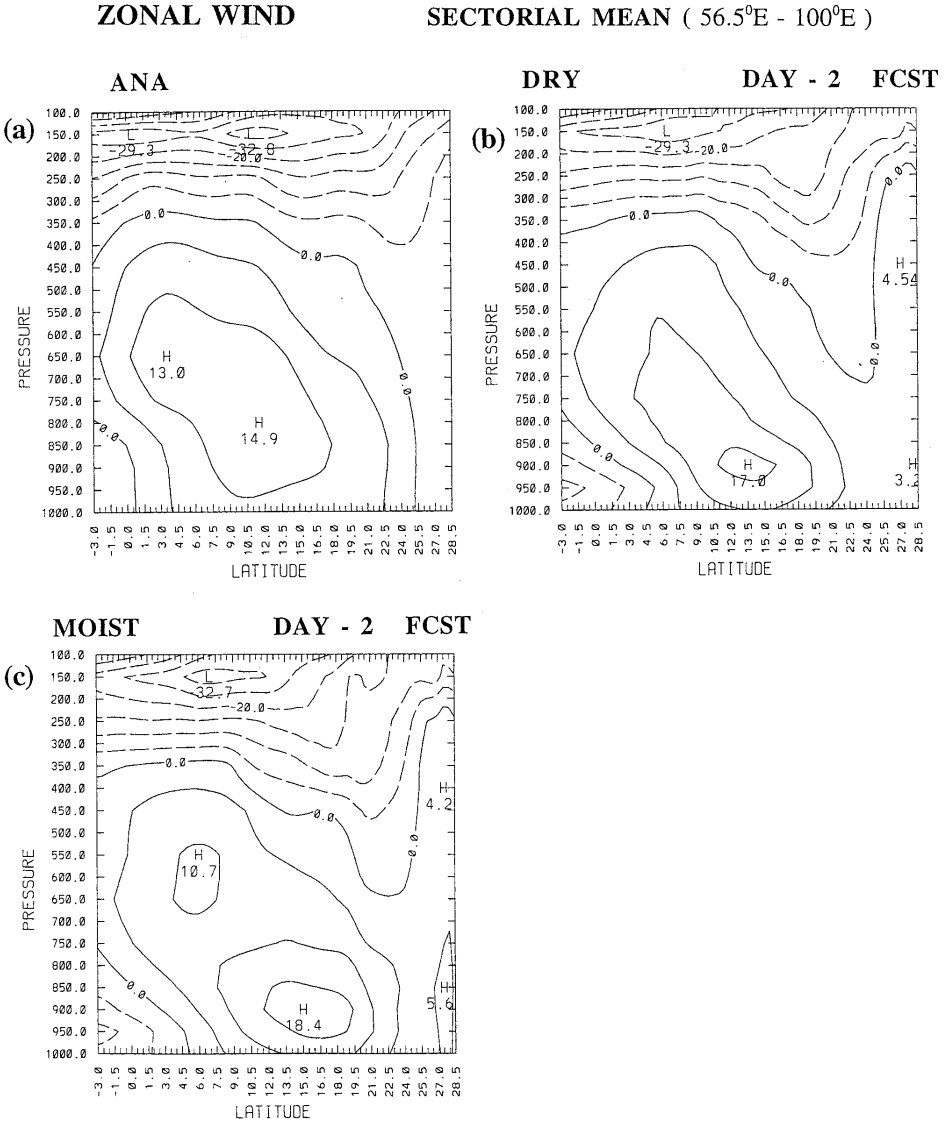

Figure 6
Latitude-height cross section of the sectorial averaged (56.5° E–100° E) zonal wind component (m s^{-1}) for fine mesh domain at 12 UTC on 14 July, 1988 for (a) ECMWF analysis, (b) DRY case and (c) MOIST case.

verifying analysis, the DRY and MOIST model runs respectively. Low-level wind maximum in the verifying analysis (Fig. 6a) corresponding to Somali jet is located at around 12°N with a value of 14.9 m s^{-1}. The observed strength of Somali jet appears to be less intense. It may be partly attributed to the coarse horizontal resolution of the analysis (1.875 latitude/longitude) and lack of adequate observations over the seas. Both DRY and MOIST cases indicate Somali jet at about 12°N with enhanced wind maxima of 17.5 m s^{-1} (Fig. 6b) and 18.4m s^{-1} (Fig. 6c), respectively. As mentioned before, wind maximum at upper levels (at 150 hPa) is due to the presence of the tropical easterly jet. A strong vertical wind shear exists from the lower troposphere to the upper troposphere over this region. This tropical easterly jet is well simulated in both DRY and MOIST cases. As expected, simulation in the MOIST case (32.7 m s^{-1}) is closer to the verifying analysis (32.8 m s^{-1}), while in the DRY case TEJ is weaker by about 3.5 m s^{-1}.

The sectorial mean (56.5°E to 100°E mean) of the analyzed meridional winds at 12 UTC on 14 July for the ECMWF analysis, and corresponding Day 2 simulations for the DRY and MOIST cases are illustrated in Figures 7a, 7b and 7c, respectively. The verifying analysis (Fig. 7a) clearly indicates a strong inflow into the monsoon land mass at low levels, and outflow at higher levels. This kind of flow pattern is typical of the summer monsoon circulation. This meridional circulation leads to low-level influx of moisture into the monsoon region with intense convective activity and an upper level strong divergent flow from the region. KRISHNAMURTI *et al.* (1983) observed that this low-level influx of moisture and the upper level strong divergent flow sustain and intensify the entire monsoon circulation and cause strong convective activity with heavy rainfall over the region.

The model simulations with DRY and MOIST cases represent the meridional circulation well. The upper level north/south return flow is stronger with MOIST case (maximum of 9.3 m s^{-1}) as compared to the verifying analysis (maximum of 6.9 m s^{-1}). DRY case predicted a maximum of 7.8 m s^{-1}.

The second-day simulation of the vertical velocity, $\dot{\sigma}$ at the first model layer (25 m above the surface) at 12 UTC on 14 July for DRY and MOIST cases is shown in Figures 8a and 8b, respectively for the fine grid model. Model simulations for both cases indicate strong rising motions along the Western Ghats, and sinking motions over the southeast coast of India. However, the rising motions along the Western Ghats are stronger with the MOIST scheme as compared to the DRY case. The maximum rising motions along the Western Ghats are -12.5 mb hr^{-1} (-3.3 cm s^{-1}) and -15.6 mb hr^{-1} (-4.4 cm s^{-1}) with DRY and MOIST cases, respectively. Strong rising motions are also predicted over eastern India with the MOIST case. These upward motions are absent in the DRY case. The regions of rising motion are consistent with convective regions and precipitation zones.

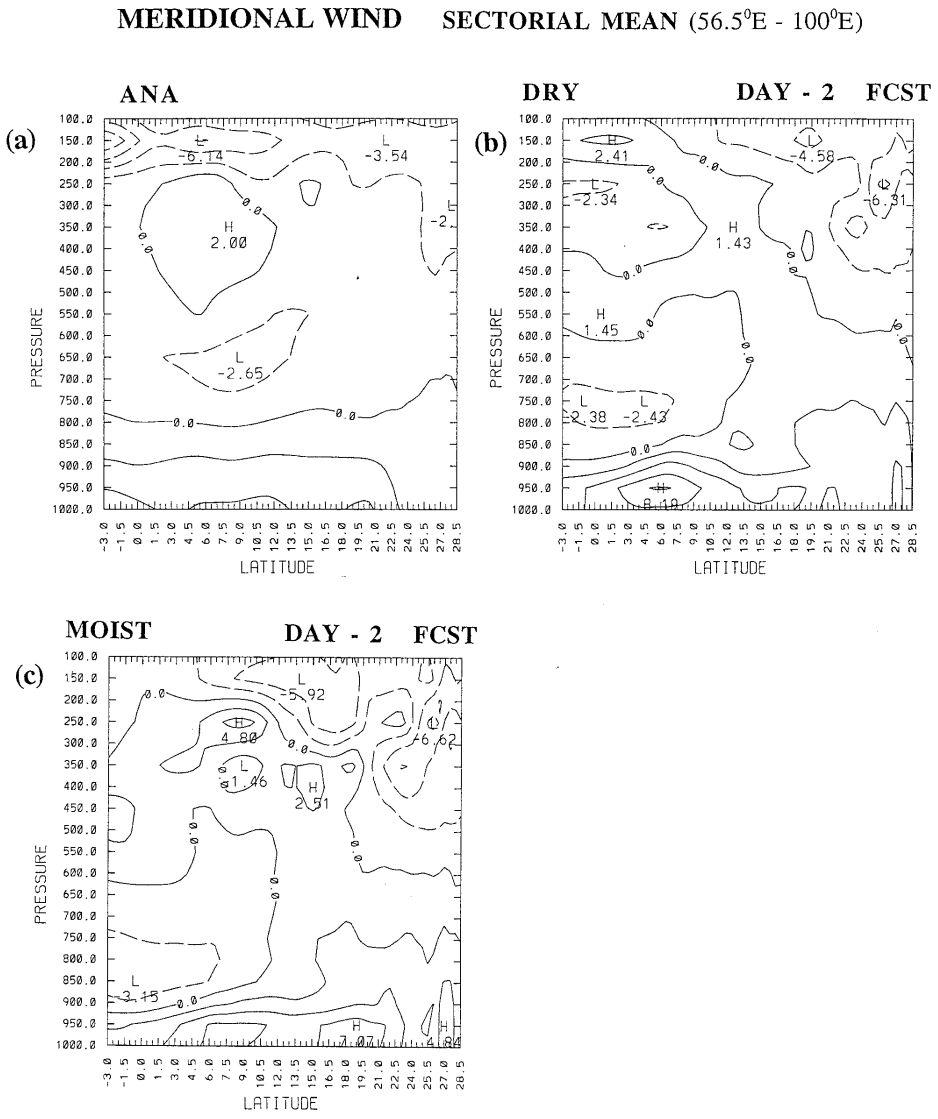

Figure 7
Latitude-height cross section of the sectorial averaged (56.5° E–100° E) meridional wind component (m s^{-1}) for fine mesh domain at 12 UTC on 14 July 1988 for (a) Verifying analysis, (b) Day-2 simulation DRY case and (c) Day-2 simulation MOIST case.

This enhanced rising motion along the Western Ghats and also over the eastern part of India in the MOIST case increased the predicted rainfall over this region (shown in a later section). The sinking motions are consistent with regions of least precipita-

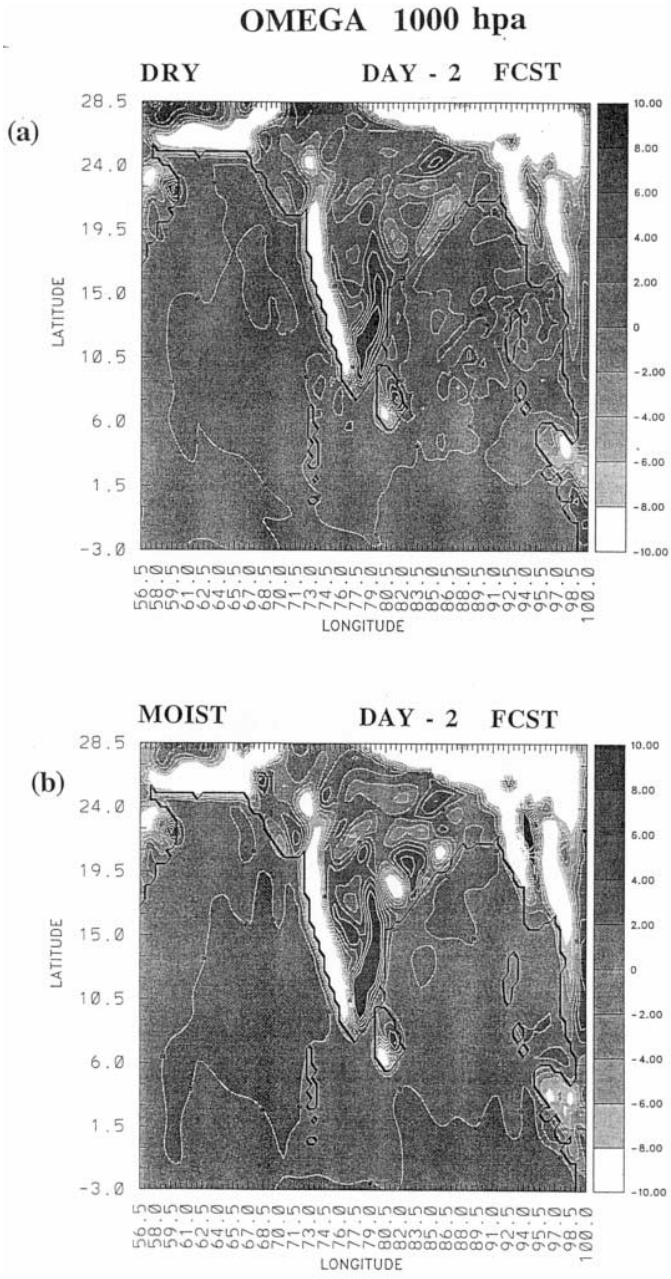

Figure 8
Predicted vertical velocities (in mb hr^{-1}) at first model layer for fine mesh domain at 12 UTC on 14 July, 1988 for (a) Day-2 simulation DRY case and (b) Day-2 simulation MOIST case.

tion such as the southeast coast of India. However, over the desert region, due to strong heating in low levels, there is rising motion in the lower troposphere with both the simulations, leading to dry convective activity over this region. As expected, in the DRY case sensible heat flux is considerable over this desert region with a maximum value of about 220 W m^{-2} and a maximum upward motion of about -3.4 mb hr^{-1} (~ 1 cm s^{-1}). However, there is a decrease in the rising motion for the MOIST case as compared to the DRY case by about 1–2 mb hr^{-1} or 0.3 cm s^{-1}. Strong descending motions are predicted over the southeast coast of India with maximum values of 8.8 mb hr^{-1} (2.5 cm s^{-1}) and 12.1 mb hr^{-1} (3.3 cm s^{-1}) with the DRY and MOIST cases, respectively.

Consistent with the horizontal wind fields, the cross section of the vertical motions also indicates a strong rising motion over land and along the Somali jet for the MOIST case as compared to the DRY model run (not shown). Along the Somali jet the maximum upward motions are about 3.7 mb hr^{-1} (1 cm s^{-1}) and 4.1 mb hr^{-1} (1.2 cm s^{-1}) for the DRY and MOIST cases, respectively.

4.2 Surface Fluxes and Rainfall

The surface latent heat flux for both DRY and MOIST model simulations at the end of 48 hr are presented in Figures 9a and 9b, respectively. For the DRY case, latent heat flux is zero over land. Over ocean, both the cases are similar, with maximum latent heat flux occurring over the region of Somali jet (210 W m^{-2}). Latent heat fluxes over land using the MOIST scheme (Fig. 9b) appear to be within the generally observed range (< 150 W m^{-2}) except over eastern India (19.5°N, 82°E) where a maximum of 250 W m^{-2} was simulated. This intensification could be due to the strong surface winds associated with the low-pressure system in this region and near saturated landmass. As expected, latent heat fluxes are very weak over the desert region in the MOIST case. Along the Western Ghat mountains latent heat fluxes are of the order of 60–90 W m^{-2} with a significant horizontal gradient. In particular, a strong heat flux gradient is observed over central India close to the monsoon trough region (Fig. 9b). These large heat flux gradients are primarily due to the inhomogeneities in vegetation and soil moisture over the region. These gradients would further increase the precipitation over this region. Observations also confirmed significant amounts of rainfall in this region.

In both the cases the latent heat fluxes along the Somali jet increased on the second day (Fig. 9) as compared to the first day (not shown). This increase in latent heat flux can be attributed to an increase in the low level wind speed along the jet on the second day.

Distribution of the surface turbulent sensible heat fluxes are illustrated in Figures 10a and 10b for the DRY and MOIST cases at the end of the 48 hr model integration. Both cases evidence strong positive gradients west of 85°E longitude and negative towards the east as expected. These negative sensible heat fluxes east

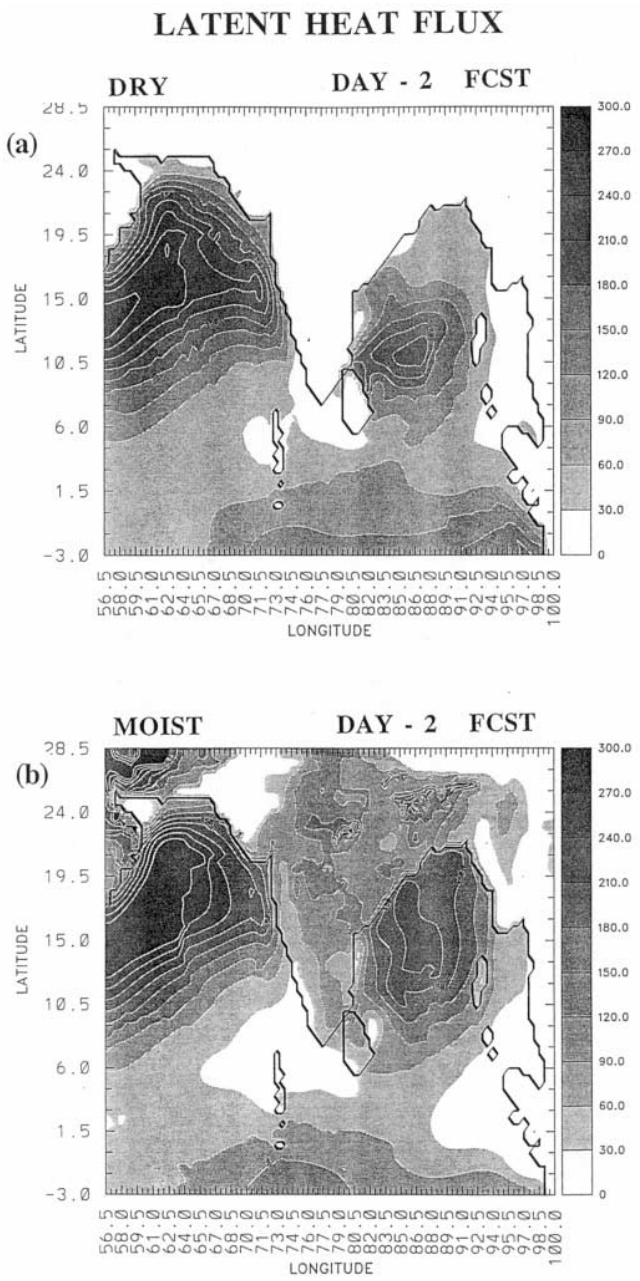

Figure 9
Predicted latent heat fluxes (W m^{-2}) for fine mesh domain at 12 UTC on 14 July, 1988 for (a) Day-2 simulation DRY case and (b) Day-2 simulation MOIST case.

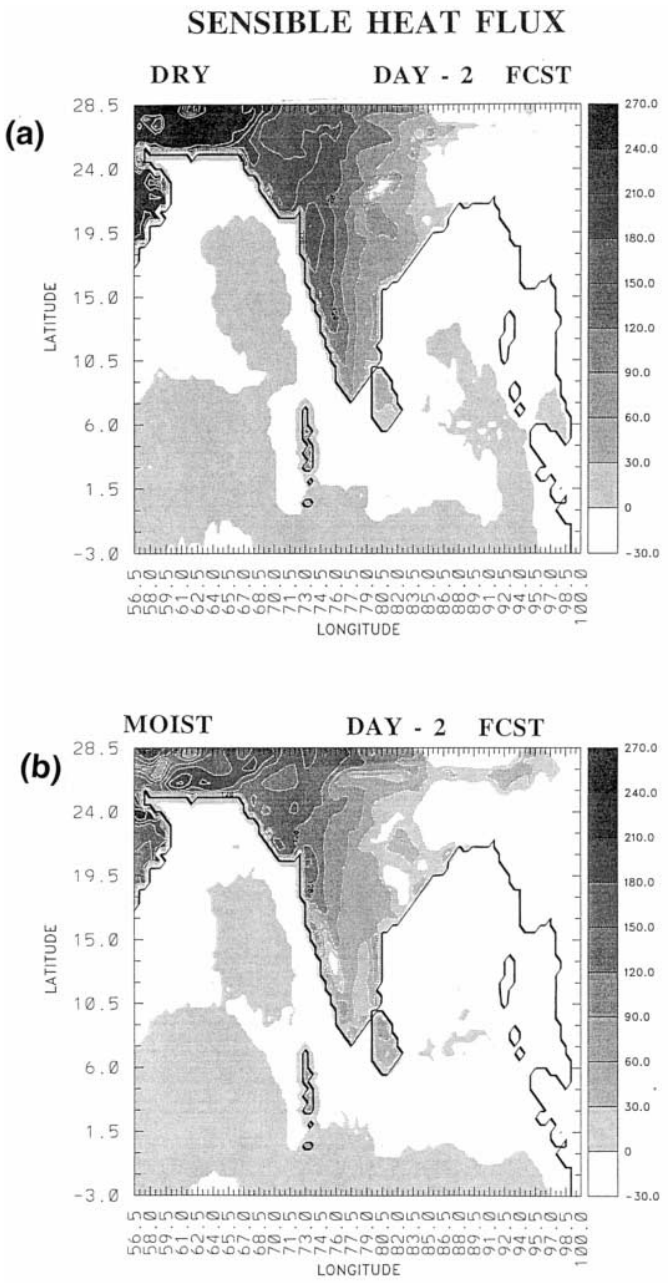

Figure 10
Predicted sensible heat fluxes (W m^{-2}) for fine mesh domain at 12 UTC on 14 July, 1988 for (a) Day-2 simulation DRY case and (b) Day-2 simulation MOIST case.

of 85°E are due to near zero incoming solar radiation at 48 hrs corresponding to 5.30 pm LST. However, for both cases, gradients appear to be reasonable over land with maximum sensible heat flux ($>$ 120 W m^{-2}) over western deserts. Sensible heat fluxes with the MOIST scheme (Fig. 10b) are small over the east coast near 19.5 N, and 82 E where the latent heat fluxes are maximum (Fig. 9b). The sensible heat fluxes are small in this region due to the decrease in ground temperature as a result of large latent heat fluxes due to the presence of vegetation cover. In general, sensible heat fluxes in the DRY case (Fig. 10a) are larger than those for the MOIST case (Fig. 10b). This could be due to an overall increase in ground temperature in the DRY case as compared to the MOIST case. The assumption of dry bare soil conditions in the DRY case with constant thermal capacity increased the ground temperature during day time and caused more cooling during nighttime.

The horizontal distribution of ground temperature for the DRY and the MOIST cases is shown in Figures 11a and 11b, respectively. As expected, predicted ground temperature in the DRY case is higher (2–4°C) as compared to the MOIST case during daytime. This could be because of the fact that the heat capacity of the bare soil is smaller than that of the vegetated land. Further, evaporation from the vegetated land tends to cool down the surface temperature.

Observed and predicted rainfall (mm d^{-1}) for the Day 1 simulation of the FGM with DRY and MOIST runs for 13 July 1988 is presented in Figures 12a, 12b and 12c, respectively. Along the west coast of India and offshore, large rainfall rates are observed. Due to the orographic lifting and associated convection, heavy rainfall occurs along the west coast of India. Maximum rainfall observed along the west coast of India is about 100 mm day^{-1} (Fig. 12a). Substantial rainfall was also observed over the central regions of India with a maximum of about 140 mm d^{-1} during the same period.

In general, both the cases predicted good rainfall distribution. As expected, high rainfall rates are predicted along the west coast of India. Along the Western Ghats the model with the MOIST scheme predicted a 90 mm day^{-1}. DRY run predicted a maximum rainfall of some 80 mm day^{-1}. Observations in this region indicated a maximum rainfall of approximately 100 mm day^{-1}. The rainfall prediction using the MOIST scheme (Fig. 12c) is comparable to observations (Fig. 12a) in both spatial extent and magnitude. In the region of the monsoon trough, where strong heat flux gradients exist, the MOIST case precipitation is larger. The maximum precipitation in this region is also consistent with the observations. Precipitation over central India is poorly simulated with the DRY model run. In summary, predicted spatial distribution of rainfall along the west coast of India and other parts of the Indian sub-continent is in better agreement with the observations (Fig. 12a) at the end of the first day with MOIST case. As expected, predicted rainfall rates are larger for the fine grid domain as compared to the coarse grid domain for all cases (not shown). However, even the MOIST model did not simulate the observed intensity and distribution of rainfall over central India. This is believed to

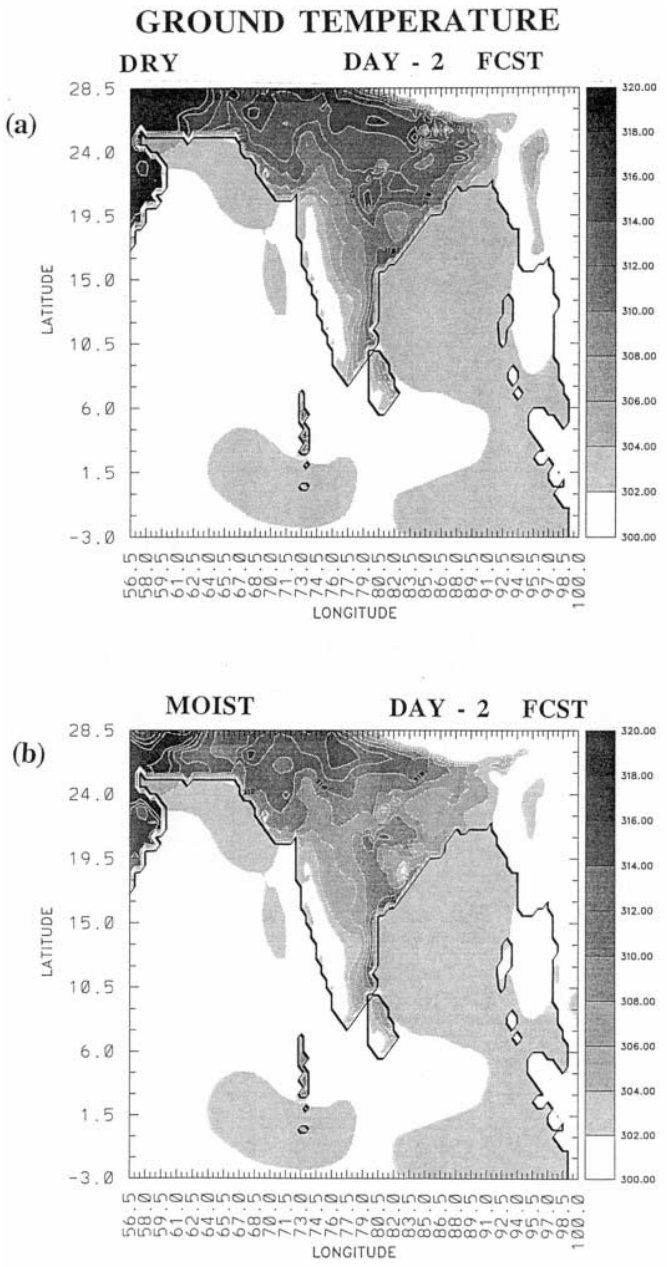

Figure 11
Predicted ground temperature (K) for fine mesh domain at 12 UTC on 14 July, 1988 for (a) Day-2 simulation DRY case and (b) Day-2 simulation MOIST case.

be due to uncertainties in the prescription of the initial surface conditions such as soil moisture and land use pattern. It is expected that an increase in the model resolution would also improve the prediction of rainfall.

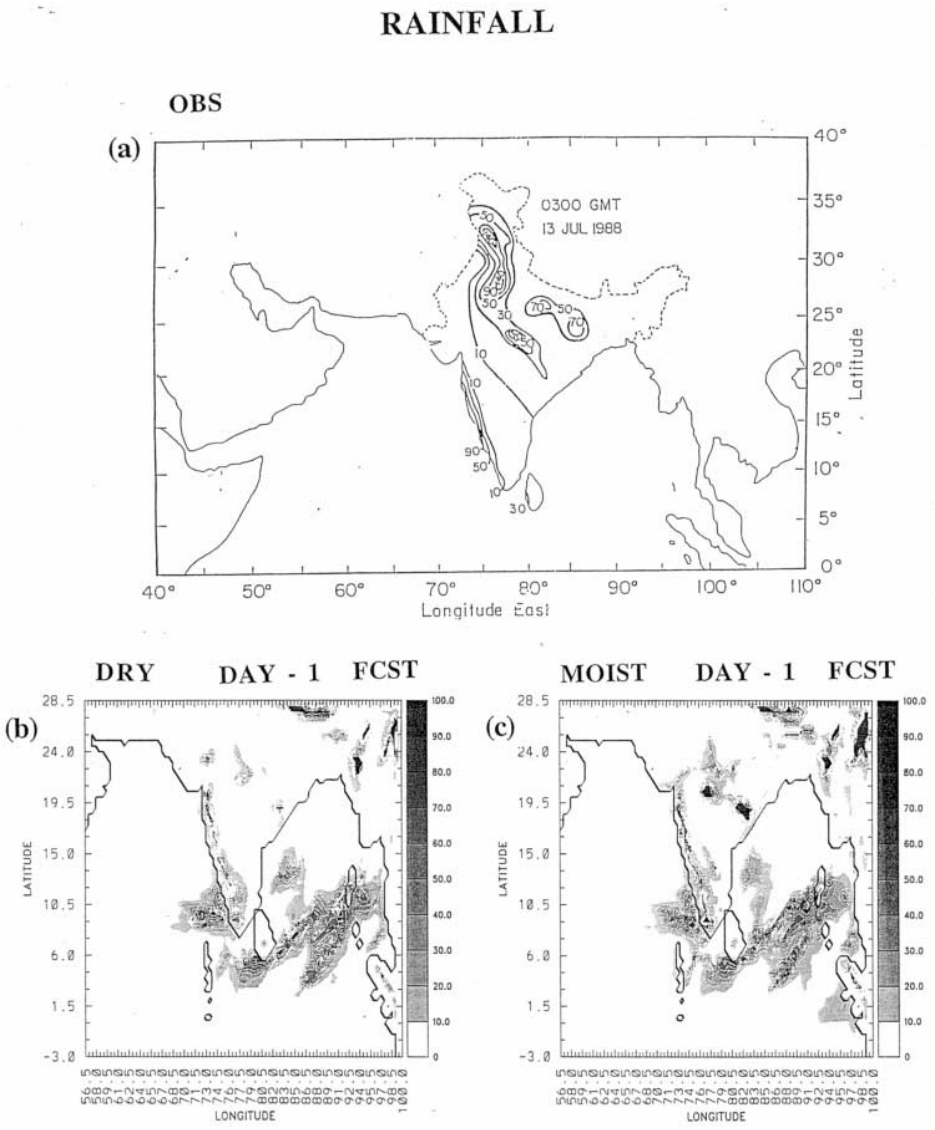

Figure 12
Observed and Day-1 predicted total rainfall distribution (mm day^{-1}) for fine mesh domain on 13 July, 1988 for (a) observations, (b) DRY case and (c) MOIST case.

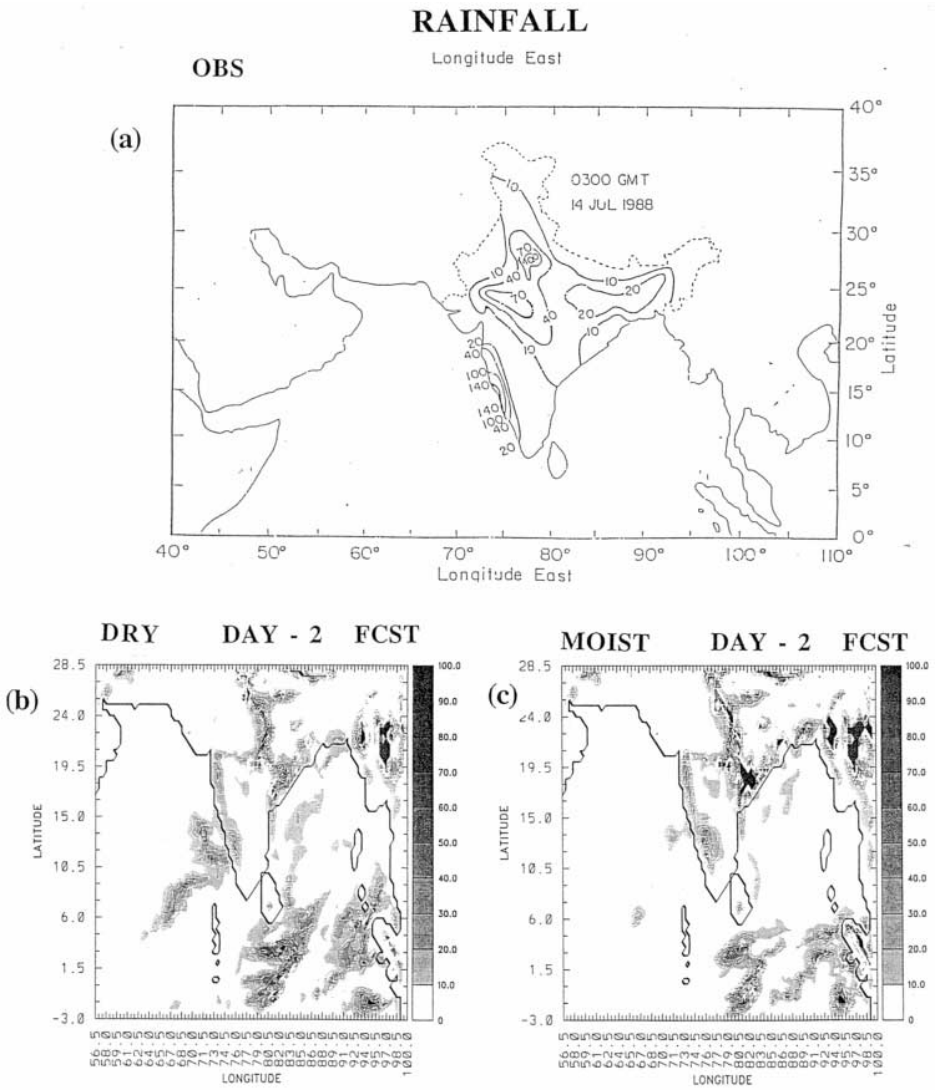

Figure 13
Observed and Day-2 predicted total rainfall distribution (mm day^{-1}) for fine mesh domain on 14 July, 1988 for (a) observations, (b) DRY case and (c) MOIST case.

The observed and the model predicted (DRY and MOIST) horizontal distribution of precipitation for Day-2 on 14 July are shown in Figures 13a, 13b and 13c, respectively. A maximum rainfall of 140 mm day^{-1} was observed (Fig. 13a) along the west coast of India on 14 July, 1988. Intense rainfall was also observed over the

central regions of India with a maximum of about 120 mm day^{-1} during this period. The predicted maximum rainfall along the Western Ghats with DRY case (Fig. 13b) is about 108 mm day^{-1}. Once again MOIST case predicted more precipitation along the Western Ghat mountains (Fig. 13c) with a maximum of about 126 mm day^{-1}. In other parts of the Indian subcontinent, especially over

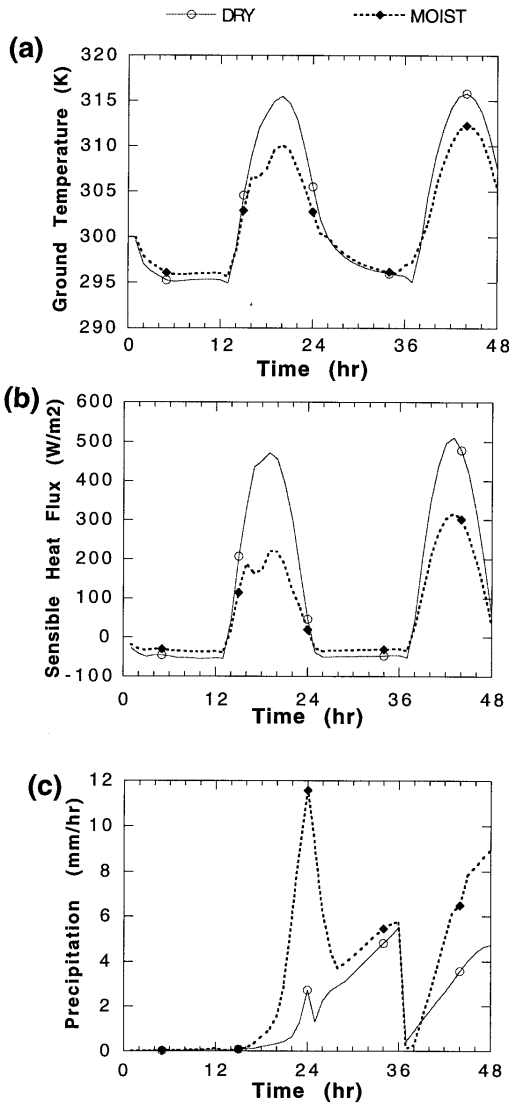

Figure 14
Diurnal variation of (a) ground temperature (K), (b) surface sensible heat flux and (c) total rainfall over peninsular India [12° N–15° N and 77° E–79° E].

central and northern India, spatial distribution and the magnitudes of predicted rainfall using the MOIST model are in agreement with the observations.

In summary, the sensitivity study using bare soil condiitons and realistic soil distributions indicates the importance of land surface processes on atmospheric mesoscale simulation. The results supply better prediction of latent and sensible heat fluxes when a soil moisture scheme (MOIST) is used. As a consequence of soil moisture availability, increased surface evaporation causes a decrease in surface temperature (a difference of about 3–4°C was predicted at daytime between the DRY and the MOIST cases), which in turn decreased the sensible heat flux. A comparison of individual water vapor fluxes from the MOIST case show a strong dependency of the energy budget on the properties of the vegetation. During the day foliage transpiration (Etr) enhances the latent heat flux in vegetated areas and consequently contributes towards the reduction of surface heating.

4.3 Diurnal Variation of Thermodynamic Variables

In this section temporal variation of ground temperature, sensible heat fluxes, latent heat fluxes and rainfall rate during the entire simulation period (48 hrs) are discussed and results from DRY and MOIST runs compared. For this purpose, two small regions are selected in the fine grid model domain. The first location is over the peninsular India [12°N–15°N and 77°E–79°E] and the second one is over the desert region in northwest India [22°N–24°N and 72°E–74°E]. The 5×7 grid points boxes are selected in these two locations, and the model output in those boxes averaged hourly to illustrate diurnal variation of these parameters.

The box averaged diurnal variation of ground temperature, sensible heat flux and precipitation over the peninsular India are shown in Figures 14a, 14b and 14c, respectively. As expected, ground temperature in the DRY case is higher during daytime (by about 3–4°C) and cooler at night (1–2°C) as compared to the one with the MOIST scheme. The thermal heat capacity of the dry bare soil is small compared to vegetated land, and as a result, the ground temperatures increase rapidly during daytime and decrease during nighttime. Hence ground temperatures are over-predicted during day time and under-predicted at night. This extensive variation in ground temperature generates large sensible heat fluxes in the DRY case. Further, evaporation from the vegetated land tends to cool the ground temperatures (MOIST case).

Sensible heat fluxes over peninsular India are shown in Figure 14b. As mentioned earlier, the substantial difference in ground temperature and air temperature in the DRY case caused large sensible heat fluxes over these regions. The results from the MOIST scheme appear to be reasonably good. The maximum and minimum fluxes are within the generally observed range over India (RAMAN *et al.*, 1990).

The predicted rainfall rate for 48 hrs simulation over peninsular India is shown in Figure 14c. As expected, rainfall rates over peninsular India are more abundant

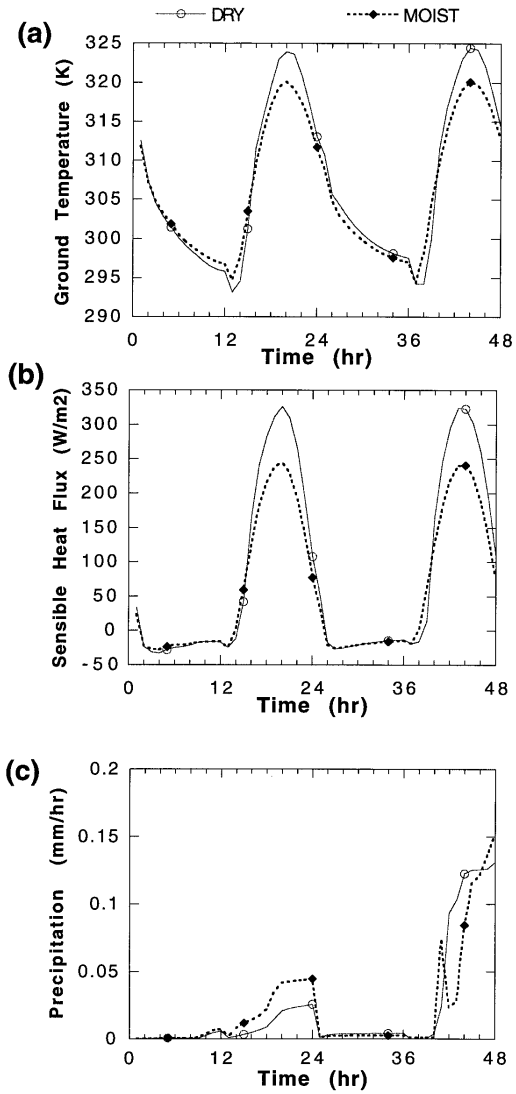

Figure 15
Diurnal variation of (a) ground temperature, (b) surface sensible heat flux (W m^{-2}) and (c) total rainfall (mm hr^{-1}) over the Desert region (Northwest India) [21° N–24° N and 72° E–74° E].

for the MOIST case compared to the DRY case. The increased rainfall rates are mainly due to the large latent heat fluxes and large vertical motions in that region for the MOIST case. The rainfall rates are about 20–30% higher in the MOIST case as compared to the DRY case. Thus an overall enhancement of the hydrological cycle is ascertained with the MOIST case.

Diurnal variation of ground temperature, sensible heat flux and precipitation over the desert region are shown in Figures 15a, 15b and 15c. Once again a diurnal variation can be seen in all these three variables. However, the precipitation over the desert region in the DRY case, though small in magnitude, is slightly higher as compared to the MOIST case. Strong rising motions were predicted in this region in both cases, but these vertical motions are slightly stronger in the DRY case as compared to the MOIST case over the desert. Increases in the vertical motions for the DRY model could be due to the increase in the sensible heat fluxes over the desert which cause strong convection and vertical motion leading to local rainfall, though small in magnitude.

5. Summary and Conclusions

Based on the numerical simulation experiments conducted to study the impact of vegetation and soil moisture characteristics on the development of mesoscale circulations during the Indian summer monsoon, the following broad conclusions can be drawn:

The main difference in the DRY and MOIST cases is the way in which evaporation flux is estimated over land. The latent heat flux is zero over land for the DRY case, but for the MOIST case a land surface process scheme is used to estimate these latent heat fluxes. Inclusion of a land surface processes scheme in the model enhanced the predicted latent and sensible heat flux gradients over land. These gradients in the latent heat fluxes over land increased the low-level convergence. These increased heat flux gradients, especially latent heat flux, further enhanced the convection and precipitation in the MOIST model. Thus it improved the hydrological cycle of the model as compared to the DRY model run and thus provided realistic diabatic forcings in the model with the MOIST case. Enhanced hydrological cycle intensified the large-scale circulation as the strengths of both the low-level Somali jet and the upper level TEJ increased for the MOIST model run. Stronger meridional circulation caused by the large-scale divergent flow and stronger vertical motion, further enhanced the evaporation. This provided better simulation of the monsoon circulation and its associated precipitation in the MOIST case and as such demonstrate the importance of the parameterization of the land surface processes in short-range prediction/simulation of summer monsoon circulation features and rainfall over India.

Acknowledgments

This study was supported by the Division of Atmospheric Sciences, National Science Foundation under grant ATM–92-12636 and the Naval Research Laboratory, Washington, D.C.

REFERENCES

ALAPATY, K., RAMAN, S., and MADALA, R. V. (1995), *Simulation of Monsoon Boundary Layer Processes Using a Regional Scale Nested Grid Model*, Boundary Layer Meteorology *67*, 407–426.

ANTHES, R. A. (1977), *A Cumulus Parameterization Scheme Utilizing a One-dimensional Cloud Model*, Mon. Wea. Rev. *105*, 207–286.

ANTHES, R. A. (1984), *Enhancement of Convective Precipitation by Mesoscale Variations in Vegetative Covering in Semi-arid Regions*, J. Climate and Applied Meteor. *23*, 541–554.

BARNSTON, A. G., and SCHICKEDANZ, P. T. (1984), *The Effect of Irrigation on Warm Season Precipitation in the Southern Great Plains*, J. Climate Appl. Meteor. *23*, 865–888.

BURMAN, R. D., WRIGHT, J. L., and MARWITZ, J. D. (1977), *Climate Modification of Dry Desert Air by a Large Irrigation Project*, 6th Conference on Planned and Inadvertent Weather Modification, Amer. Meteor Soc., Champaign-Urbana, 81–82.

CLAPP, R., and HORNBERGER, G. (1978), *Empirical Equations for Some Soil Hydraulic Properties*, Water Resour. Res. *14*, 601–604.

DICKINSON, R., HENDERSON-SELLERS, A., Kennedy, P., and Wilson, M. (1986), *Biosphere-Atmosphere Transfer Scheme (BATS) for the NCAR Community Climate Model*, NCAR/TN-275 + STR, 69 pp.

GARRETT, A. J. (1982), *A Parameter Study of Interactions between Convective Clouds, the Convective Boundary Layer, and a Forested Surface*, Mon. Wea. Rev. *110*, 1041–1059.

HENDERSON-SELLERS, A. (1993), *A Factorial Assessment of the Sensitivity of the BATS Land-surface Parameterization Scheme*, J. Climate *6*, 227–247.

HONG, X., LEACH, M. J., and RAMAN, S. (1995), *A Sensitivity Study of Convective Cloud Formation by Vegetation Forcing with Different Atmospheric Conditions*, J. Appl. Meteor. *34*, 2008–2028.

KRISHNAMURTI, T. N., COCKE, S., PASCH, R., and LOW-NAM, S. (1983), *Precipitation Estimates from Raingage and Satellite Observations: Summer MONEX*, Dept. of Meteorology, Florida State University, 373 pp.

KUO, H. L. (1974), *Further Studies of the Parameterization of the Influence of Cumulus Convection on Large-scale Flow*, J. Atmos. Sci. *31*, 1232–1240.

MADALA, R. V., CHANG, S. W., MOHANTY, U. C., MADAN, S. C., PALIWAL, R. K., SARIN, V. B., HOLT, T., and RAMAN, S. (1987), *Description of the Naval Research Laboratory Limited Area Dynamical Weather Prediction Model*, NRL Memo. Rep. No. *5992*, Naval Research Laboratory, Washington, D.C., 131 pp.

MAHFOUF, J.-F., RICHARD, E., and MASCART, P. (1987), *The Influence of Soil and Vegetation on the Development of Mesoscale Circulations*, J. Clim. Appl. Met. *26*, 1483–1495.

MATTHEWS, E. (1984), *Vegetation, Land-use and Albedo Data Sets*, NASA Tech. Memo. *86107*.

MCCUMBER, M. C. (1980), *A Numerical Simulation of the Influence of Heat and Moisture Fluxes upon Mesoscale Circulations*, Report UVA-ENV SCI-MESO-1980-2, Dept. of Environmental Science, University of Virginia, 255 pp.

NOILHAN, J., and PLANTON, S. (1989), *A Simple Parameterization of Land-surface Processes for Meteorological Models*, Mon. Wea. Rev. *117*, 536–549

OOKOUCHI, Y., SEGAL, M., KESSLER, R. C., and PIELKE, R. A. (1984), *Evaluation of Soil Moisture Effects of the Generation and Modification of Mesoscale Circulations*, Mon. Wea. Rev. *112*, 2281–2292.

OTTERMAN, J. (1974), *Baring High Albedo Soils by Overgrazing: A Hypothesized Destrification Mechanism*, Science *196*, 531–533.

RAMAN, S., TEMPLEMAN, B., TEMPLEMAN, S., MURTHY, A. B., SINGH, M. P., AGARWAAL, P., NIGAM, S., PRABHU, A., and AMEENULLAH, S. (1990), *Observation of Mean Boundary Layer Structure and Turbulence During Pre-monsoon and Monsoon Periods in India*, Atmospheric Environment *24*A, 723–734.

SELLERS, P., MINTZ, Y., SUD, Y., and DALCHER, A. (1986), *A Simple Biosphere Model (SiB) for Use with General Circulation Models*, J. Atmos. Sci. *43*, 505–531.

XU, L., RAMAN, S., MADALA, R. V., and HODUR, R. (1996), *A Non-hydrostatic Modeling Study of Surface Moisture Effects on Mesoscale Convection Induced by Sea Breeze Circulation*, Meteorol. and Atmos. Phys. *58*, 103–122.

ZHANG, D., and ANTHES, R. A. (1982), *A High-resolution Model of the Planetary Boundary Layer—Sensitivity Tests and Comparisons with SESAME-79 Data*, J. Appl. Meteor. *21*, 1594–1609.

(Received June 17, 1997, accepted June 19, 1998)